

Construction and Evaluation of a Graphene Oxide Functionalized Aminopropyltriethoxy Silane Surface Molecularly Imprinted Polymer Potentiometric Sensor for Dipyrnidamole Detection in Urine and Pharmaceutical Samples

Roya Mirzajani^{1b}*^a and Ehsan Arefiyan^a

^aChemistry Department, College of Science, Shahid Chamran University of Ahvaz, 31587-77871 Ahvaz, Iran

A dipyrnidamole (DIP) based surface molecularly imprinted polymer (MIP) was synthesized and applied as a sensing agent in a sensing layer of a new modified potentiometric carbon paste electrode (CPE). The potentiometric modified CPEs (GO@SiO₂-NH₂-MIP/MWCNTs/CPE, where GO is graphene oxide and MWCNTs is multi-walled carbon nanotubes) showed an improved performance in term of Nernstian slope, selectivity and response time compared to the unmodified CPE. The response time of the sensor in the range of 2.5×10^{-8} - 1.1×10^{-2} M DIP was 20 s. The obtained DIP sensor showed low limit of detection (1×10^{-8} M), and satisfactory long-term stability (higher than 4 months). The practical application of the sensor was demonstrated by the determination of DIP concentration in urine samples and pharmaceutical preparations, with good precision and acceptable recoveries (96.0-103.0%). The prepared sensor showed high selectivity for DIP over a number of common species (aspirin, caffeine, ascorbic acid, glucose, urea, bipyridine, Na⁺, Fe³⁺, Mg²⁺, Ca²⁺ and K⁺).

Keywords: dipyrnidamole, potentiometric sensor, carbon paste electrode, graphene oxide, imprinted polymer

Introduction

Dipyrnidamole (DIP) 2,29,29,2-[(4,8-dipiperidino-pyrimino [5,4-*d*] pyrimidine-2,6-diyl) dinitrilo] tetraethanol (Figure 1) is a well-known vasodilator drug that has been widely used for treatment of coronary heart diseases,¹ and a classic platelet inhibitor being a key medicine in clinical therapy of thrombosis and cerebrovascular disease. This drug possesses pleiotropic anti-inflammatory, anti-proliferative and anti-oxidant actions.² A number of clinical and experimental studies highlights the renoprotective potentials of dipyrnidamole. For instance, dipyrnidamole and aspirin treatment, either alone or in combination, reduces proteinuria in diabetic patients with nephropathy. Dipyrnidamole at high-dose is proischemic, and could cause a coronary steal effect.

On the other hand, oral low-dose dipyrnidamole could have a minimal hemodynamic effect.^{3,4} This antithrombotic drug is quickly absorbed after oral administration and is eliminated mainly in the feces, although the excretion may be delayed due to the enterohepatic circulation. Small amounts are excreted in the urine as the glucuronide

conjugate. After a single 100-mg oral dose of this drug given to a normal healthy volunteer, the concentration in plasma varies from about 1526 ng mL⁻¹ after 1 h medication to about 116 ng mL⁻¹ after 12 h (the half life time in plasma).⁵ Owing to increasing of energy production that the vasodilator can produce, it is classified in doping terms as a stimulant. Dipyrnidamole is widely used in medicine, but it has a fraudulent consumption in certain sports, with the purpose of increasing efficiency and decreasing tiredness. Unfortunately, the excessive consumption of DIP could cause mental illness and serious side effects.⁶ Thus, it is essential and valuable to monitor the DIP concentration in biological samples.

DIP detection in biological and tablets/injections samples has been performed using various analytical methods including spectrophotometry,⁷ fluorescence spectrometry,⁸ high performance liquid chromatography (HPLC),^{9,10} extraction-gravimetry modified surface,¹¹ differential pulse adsorptive stripping voltammetry (DPASV),¹² square wave voltammetry,¹ chemiluminescence (CL) sensor,¹³⁻¹⁵ molecularly imprinted polymer (MIP)-modified electrode differential pulse voltammetry.^{16,17}

The common technique applied in the DIP determination is HPLC method.¹⁸ HPLC method has many advantages, but

*e-mail: rmirzajani@scu.ac.ir

one serious problem for the determination of the analyte is complicated in the preliminary procedures, such as extraction.¹⁹ Despite the simplicity of spectrophotometric methods, they are not very sensitive and often subject to interference from other analytes. However, some of the other methods are expensive, time-consuming or have limited sensitivity. The present investigation was prompted by the need to develop more reliable, selective, sensitive, simple, fast and less time-consuming methods for quantitative analysis of the drug.

Sensors have capability to transform physical or chemical information from their environment into a signal that can later be processed. Electrochemical sensors are among the most widely used devices and one of these being the potentiometric sensor.²⁰⁻²² Ion-selective electrodes (ISEs) with polymeric membranes containing selective carriers (ionophores) are the most commonly-used potentiometric sensors.²³ They have been widely used for directly determining various inorganic and organic ions in medical, environmental and industrial analyses. Over the past two decades, imprinted polymers have attracted broad interest from scientists appointed in electrochemical sensor development.^{24,25}

The molecular imprinting technique is a powerful method for preparing artificial recognition sites with predetermined selectivity for a wide range of target molecules.^{26,27} The presence of nanomaterials in MIP sensors has boosted the advances in sensitivity enhancement owing to the specific binding sites forming predominantly at the material surface, as well as regular morphology, large surface and good stability.^{25,28} In the surface imprinted materials, as the imprinted sites are close to or at the surface of MIPs, the binding and rebinding of the target compounds could be achieved easily.²⁹

Graphene oxide (GO) has been recently considered as an ideal candidate as supporting material for preparing surface molecularly imprinted composites. Although graphene oxide is not electrically conductive, the significant amount of oxygen functional groups, as well as its negative charge, makes it ionically conductive.^{30,31} Thus, GO is potentially useful in solid state ion-selective electrodes, in which conduction is ionic rather than electronic.³² The adjustable functional groups (i.e., hydroxyl, carboxyl and epoxide groups), high surface area, excellent mechanical properties and good compatibility with polymers have made GO as promising material to synthesize nanocomposites.³³ By using GO as the supporting material of MIP layer, the detection sensitivity could be improved in terms of accelerating the ionic transfer rate and specific surface area. The integration of electrochemical devices and MIPs is an attractive method for the development of biochemical sensors, which demonstrates both good sensitivity and selectivity.

This work describes the preparation of a new graphene oxide based surface MIP modified carbon paste electrode (CPE). In the present work, instead of the methods described above, we propose a selective and sensitive sensor for simple, fast and direct dipyrindamole determination in pharmaceutical formulation and biological fluids like urine samples, without the need for prior separation, preconcentration or the derivation procedures. These properties mean that this sensor is totally available in routine analysis. Actually it is the first application of GO@SiO₂-NH₂-MIP/MWCNTs/CPE (where MWCNTs is multi-walled carbon nanotubes) in the literatures and there is not any report about the application of this electrode for the potentiometric determination of other compounds. The proposed sensor presented good limit of detection (LOD) and wide linear range in comparison to the former reports for electrochemical determination of DIP.

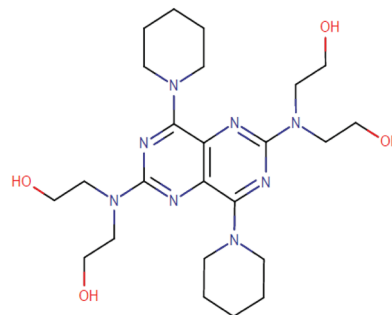


Figure 1. Chemical structure of dipyrindamole (DIP).

Experimental

Instrumentation

A Metrohm pH-meter (827 pH lab, Metrohm, Herisau, Switzerland) with a combined glass electrode was used for the potential and pH measurements. A Heidolph type of stirrer (MR 2000, Germany) was used for stirring the solutions. The morphology and structure of the synthesized GO, GO@SiO₂-NH₂ and polymers were characterized by scanning electron microscopy with energy dispersive X-ray spectroscopy (SEM-EDX, XL30, Philips, Netherland). Fourier transform infrared (FTIR) spectra of GO, GO@SiO₂-NH₂ and GO@SiO₂-NH₂-MIP composites were recorded on a Spectrum GX FTIR Spectrometer (PerkinElmer Inc., USA), using KBr pellets in the range of 400-4000 cm⁻¹.

Reagents and materials

All the chemicals and reagents used in this work were of analytical grade and used without further

purification. Dipyridamol ($C_{24}H_{40}N_8O_4$, molecular weight of $504.626 \text{ g mol}^{-1}$, Figure 1) was purchased from Sigma-Aldrich (St. Louis, MO, USA). Graphite powder, pure silicon oil and MWCNTs (10-40 nm diameters, 95% purity) were all purchased from Merck (Darmstadt, Germany) and were used for preparation of conventional carbon paste electrode. 3-Aminopropyl triethoxy silane (APTES), methacrylic acid (MAA), ethylene glycol dimethylacrylate (EGDMA) and 2,2-azobisisobutyronitrile (AIBN) were purchased from the Sigma-Aldrich. *N,N*-Dimethylformamide (DMF), ethanol, acetic acid and acetonitrile were purchased from Sigma-Aldrich. A stock solution of DIP ($50 \mu\text{g mL}^{-1}$) was prepared by dissolving appropriate amount of it in analytical pure grade methanol, and then, diluted with distilled water and stored at $5 \text{ }^\circ\text{C}$ in the dark. The dilute solutions were daily prepared with solutions composed of methanol-water aqueous solutions. A 2.0 mol L^{-1} HCl and /or $0.1\text{-}1.0 \text{ mol L}^{-1}$ NaOH solution (Merck) was used as pH adjusting. All other chemicals of analytical grade were ordered and used without further purification.

Synthesis of $\text{GO@SiO}_2\text{-NH}_2\text{-MIP}$ composite

Preparation of graphene oxide

Graphene oxide (GO) was prepared by using the Hummers method,³⁴ followed by ultrasonication for exfoliation of the graphite oxide in an organic solvent to produce graphene oxide sheets. Expandable graphite (2.5 g) was added into a 250 mL flask containing concentrated H_2SO_4 (57.5 mL). The flask was placed in an ice bath to keep the temperature at $0 \text{ }^\circ\text{C}$, and the mixture was stirred for 30 min. KMnO_4 (7.5 g) was then slowly added into the mixture with stirring and cooling to keep the temperature below $20 \text{ }^\circ\text{C}$. Afterwards, the mixture was stirred at $35 \pm 3 \text{ }^\circ\text{C}$ for 30 min. Distilled water (115 mL) was then added into the flask, the mixture was heated to $95 \text{ }^\circ\text{C}$, and held at $95 \text{ }^\circ\text{C}$ for 15 min. Finally, the reaction was terminated by addition of distilled water (350 mL) and 30% H_2O_2 solution (25 mL). The mixture was filtered, and washed with 5% HCl aqueous solution until sulfate could not be detected by BaCl_2 . The prepared graphite oxide suspension was exfoliated into the GO using an ultrasonic bath with a power of 300 W for 30 min at room temperature followed by centrifugation at 6000 rpm for 40 min to remove nonexfoliated graphite oxide. The product was dried at room temperature overnight.

APTES coated graphene oxide sheets ($\text{GO@SiO}_2\text{-NH}_2$)

APTES-functionalized GO ($\text{GO@SiO}_2\text{-NH}_2$) was made using the reaction between carboxylic acid groups and

amino groups. This synthesis was carried out at $70 \text{ }^\circ\text{C}$ for 4 h, anhydrously under nitrogen to prevent the hydrolysis of the alkoxy groups in the silane. First, ca. 500 mg of GO synthesized in the previous stage was dispersed into 200 mL of DMF. Next, 650 mg of APTES were added dropwise to the mixture. Thereafter, the obtained mixture was refluxed under nitrogen protection, at $30 \text{ }^\circ\text{C}$ for 3 h, and then at $100 \text{ }^\circ\text{C}$ for 3 h. After the reaction, the amino-GO ($\text{GO@SiO}_2\text{-NH}_2$) was purified by washing with toluene at least 3 times to remove the residual of reactants. Black solid APTES coated graphene oxide sheets were obtained after drying in the vacuum at $50 \text{ }^\circ\text{C}$ overnight.

Preparation of DIP-imprinted and non-imprinted polymer (NIP) particles

The imprinting of DIP molecules on the obtained APTES coated graphene oxide sheets was achieved by the following method. A mixture of 20 mL of acetonitrile, 0.4 mM DIP and 200 mg $\text{GO@SiO}_2\text{-NH}_2$ at $0\text{-}2 \text{ }^\circ\text{C}$ for 12 h leads to the formation of modified $\text{GO@SiO}_2\text{-NH}_2$ self-assembled by DIP. To this mixture, the cross-linker (EGDMA, 4 mM) was added. To prepare the pre-assembled solution, the reaction mixture was stirred while sealing, shaking and purging with argon gas atmosphere for 30 min. Afterwards, 20 mL of acetonitrile solution containing 40 mg of initiator (AIBN) were added to the reaction mixture upon sonication, and the solution was purged using argon gas in an ice bath for 15 min. The polymerization was carried out at $65 \text{ }^\circ\text{C}$ in an oil bath under argon gas atmosphere for 18 h. In order to verify the releasing of template molecules from the texture of the synthesized polymer, the product was isolated and washed with a mixture of solvents (methanol/acetic acid, 9:1, v/v) for several times until the DIP molecules were not detected in the washing solution. The primary experiments show that the synthesized $\text{GO@SiO}_2\text{-NH}_2\text{-MIP}$ composite adsorbent has high adsorption capacity and selectivity for the template molecule. To synthesize the non-imprinted polymers ($\text{GO@SiO}_2\text{-NH}_2\text{-NIP}$), the same synthetic procedure mentioned above was used without addition of DIP. The schematic procedure of preparing $\text{GO@SiO}_2\text{-NH}_2\text{-MIP}$ composite is shown in Figure 2.

Preparation of modified carbon paste sensor

The modified carbon paste electrodes containing $\text{GO@SiO}_2\text{-NH}_2\text{-MIP}$ as sensing agent for DIP were generally prepared by mixing certain amount of graphite powder (55%), $\text{GO@SiO}_2\text{-NH}_2\text{-MIP}$ (12%) and MWCNTs (10%) in an ultrasonic bath for at least 10 min until the modifiers were uniformly dispersed through the graphite powder. Then, pasting liquid, silicon oil (23%), was added to the mixture, and mixed again until a uniform paste was

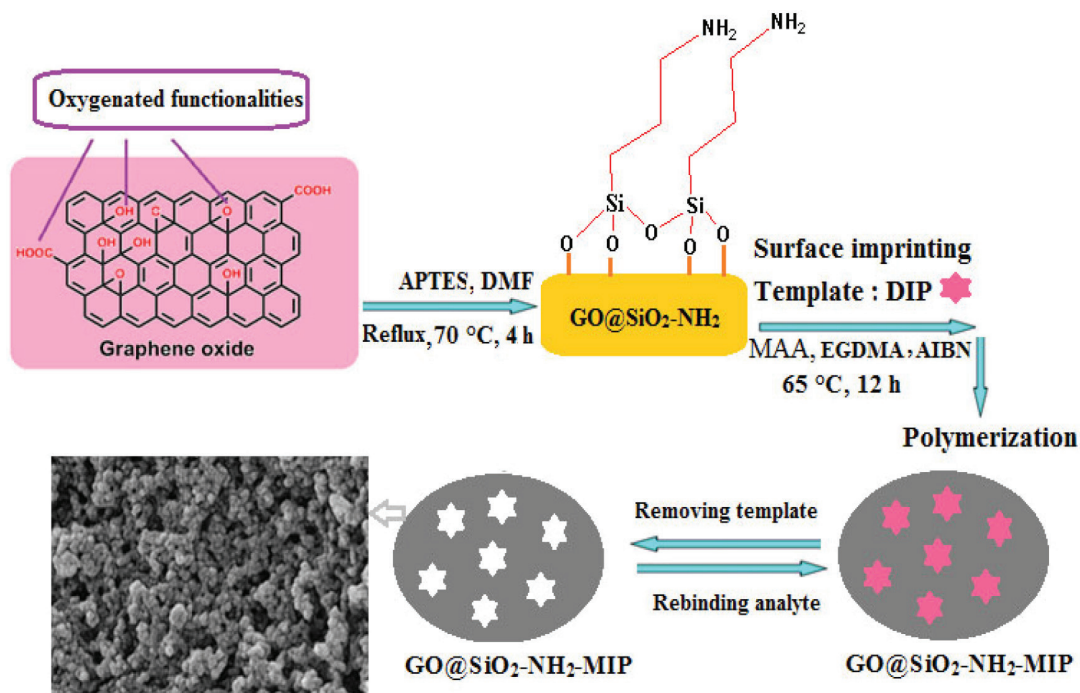


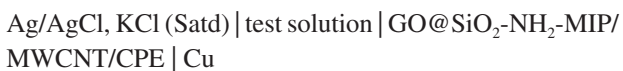
Figure 2. Synthesis of dipyrindamole (DIP)-imprinted polymer composite (GO@SiO₂-NH₂-MIP).

obtained. The paste was packed in the end of a disposable polyethylene syringe (3 mm i.d.), whose tip had been cut off with a razor blade. Electrical contact to the carbon paste was made with a copper wire. Fresh surface was obtained by applying manual pressure to the piston. The resulting fresh surface was polished on a white paper until the surface became a shiny surface. Similarly, NIP based CPE (GO@SiO₂-NH₂-NIP/MWCNTs/CPE) was prepared for comparative study.

The bare CPE without GO@SiO₂-NH₂-MIP and MWCNTs was prepared by hand mixing of 70% graphite powder and 30% silicon oil for about 10 min until a homogeneous paste was obtained. The paste was then packed into a cavity of polyethylene syringe of 3 mm internal diameter and smoothed on a tissue paper. The electrical contact was provided by a copper wire connected to the end of the tube.

Potential measurements

All potential measurements with the GO@SiO₂-NH₂-MIP/MWCNTs/CPE were carried out with the following cell assembly:



A Metrohm 827 pH-meter was used for the potential measurements. The emf (electromotive force) observations

were made relative to a silver/silver chloride electrode containing saturated solution of KCl.

DIP solutions were added to 20 mL of 0.05 M HCl solution to cover the concentration range in the range of 2.5×10^{-8} - 1.1×10^{-2} M and the potential values were recorded after each addition. Calibration graphics were then constructed by plotting the recorded potentials vs. $(-\log [\text{DIP}])$. The graphics were obtained and employed in the characterization of the slope and linear range of CPE and also subsequent determination of unknown concentration of DIP in pharmaceutical dosage and urine samples.

Preparation of real samples

Potentiometric assay of pharmaceutical preparation

Pharmaceutical sample solution was prepared by contents of 20 tablets or capsules of dipyrindamole (25 mg *per* tablet; Tolidaru Co., Tehran, Iran) that were individually weighed in order to find the average mass of each tablet and powdered or evacuated. Then, a portion of powders equivalent to the weight of one tablet was dissolved in 100 mL of phosphate buffer with sonication for 20 min. Afterward, the solution was filtered through a 0.45 μm milli-pore filter (Gelman Sciences, Rossdorf, Germany). The filtrate was subsequently diluted to volume with solvent (as in standard solution, water-methanol 1:1) to match the linear detection range of the method. The DIP content of the solution was then determined by the

proposed GO@SiO₂-NH₂-MIP/MWCNT/CPE, using the calibration graph.

DIP determination in urine samples

Urine samples were obtained from a healthy volunteer who took a single oral dose of a commercially available tablet (Tolidardu Co., Tehran, Iran) containing 25 mg of DIP. The urine samples were collected over specified time intervals (6-18 h) after the oral administration of the tablet. The samples were centrifuged for 15 min at 4000 rpm. Afterwards, 100 μ L of the clear supernatant were transferred to another centrifuge tube and the general procedure described in the proposed method was followed. Blank urine was collected from the same volunteer directly before the tablet was administered.

HPLC analysis

The chromatographic analysis was performed using a Eurosphere column (C18, 250 \times 4.6 mm) at room temperature (25 $^{\circ}$ C) with a mobile phase consisting of A (0.01 M KH₂PO₄, pH 2.5) and B (acetonitrile) in the ratio of 10 and 90% (v/v), respectively, in the isocratic mode, at a flow-rate of 0.5 mL min⁻¹. The mobile phase was filtered through a 0.22 μ m filter and degassed ultrasonically for 15 min before use. Under these conditions, the retention time for the chromatographic peaks was 5.5 min. The injection volume was 20 μ L and a wavelength of 280 nm was selected for the detection of the analyte. During the analysis, the temperature of the oven was set at 30 $^{\circ}$ C.

Results and Discussion

The GO@SiO₂-NH₂ surface can easily be modified and react with different groups for bioconjugation. During surface molecular imprinted polymer synthesis, good interactions between monomer and template represent a preliminary essential condition to obtain MIP networks with potential recognition sites. The template is assumed to interact by a combination of electrostatic interactions, π - π interactions and hydrogen bonds with monomer prior to polymerization, and after polymerization with the functional groups of the polymer matrix.²⁵ However, the extent of template-monomer interaction is influenced after polymerization by the number of monomers attached and the availability of the functional groups on the monomers. However, when the target molecule has Lewis functional group, their interaction with metacrylic acid and ethylene glycol dimethacrylate can be hydrogen bonding.

The use of immobilized templates prevents the residual template leakage and enhances the imprinting efficiency. In this work, the surface amino groups of GO@SiO₂-NH₂

were used for immobilization of the template molecules on the surface and additionally to react with the terminal vinyl groups of cross-linker, ethylene glycol dimethacrylate (EGDMA) by the Michael addition reaction.³⁵ In such a way, the imprinting sites of DIP formed on the substrate were increased. The different steps for the synthesis of GO@SiO₂-NH₂-MIPs are illustrated in Figure 2. To check the affinity of GO@SiO₂-NH₂-MIP/MWCNT as a selective modifier, a modified CPE electrode was prepared and individually used for detection of various analytes. The potential responses are shown in Figure 3. As seen, among different tested compounds, DIP with the most sensitive response seems to be determined with the constructed electrode. This is due to the selective behavior of the GO@SiO₂-NH₂-MIP/MWCNT/CPE system respect to DIP in comparison to other targets tested.

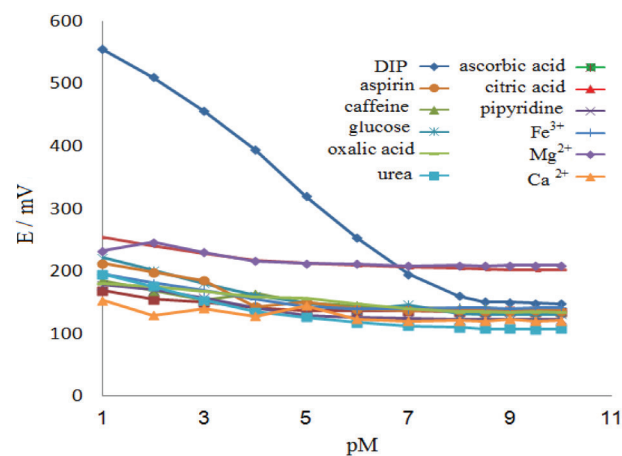


Figure 3. Potentiometric responses of the GO@SiO₂-NH₂-MIP/MWCNTs/CPE vs. some different species.

Characterization of the GO@SiO₂-NH₂-MIP composite

FTIR spectroscopic analysis

In order to confirm the synthesis of the expected products, FTIR spectra of GO, GO@SiO₂-NH₂ and GO@SiO₂-NH₂-MIPs were obtained (Figure 4). The spectrum of GO (Figure 4a) shows the peaks of -OH (3418 cm⁻¹) ascribed to the stretching of O-H, characteristic stretching vibration peak of C=O at 1725 cm⁻¹, and the peak at 1610 cm⁻¹ (sp²-hybridized C=C) can be assigned to the skeletal vibrations of graphene sheets. Figure 4b shows the FTIR spectrum of GO@SiO₂-NH₂. The sharp intense peak at 1470 cm⁻¹ can be related to the carboxylic CO group after modification with APTES. The GO silanization was confirmed via the symmetric and asymmetric Si-O-Si vibration peaks observed at 1042.06 and 1171.65 cm⁻¹, respectively. The two peaks at 1608.0 and 2800-3000 cm⁻¹ corresponding

to the N–H bending vibration and stretching vibration of C–H bonds of the methyl or methylene groups of APTES, respectively, are clearly observed in Figure 4b, confirming the surface modification of GO by APTES. As shown in Figure 4c, the characteristic absorbance band at 1731 cm^{-1} is related to direct grafting of carbonyl group of EGDMA on the surface of amino modified GO sheets. It revealed that the polymerization process was successful. In addition, the C=O peak in conjugated esters, such as EGDMA, appears in the region of $1710\text{--}1720\text{ cm}^{-1}$. The shift of C=O peak to 1731 cm^{-1} can indicate the elimination of the conjugated bond of the carbonyl group by Michael addition reaction and polymerization process.³⁶

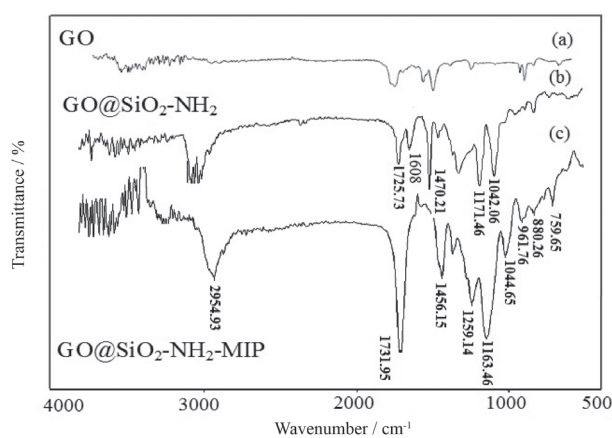


Figure 4. FTIR spectra of synthesized (a) GO, (b) GO@SiO₂-NH₂ and (c) GO@SiO₂-NH₂-MIP.

SEM and EDX characterizations

The structure, morphology and size of GO and GO@SiO₂-NH₂-MIPs were further confirmed by SEM. According to the SEM image of GO (Figure 5a), the prepared GO represents a layered and sheet-like structure with the large surface and wrinkled edge. This wrinkled nature of GO provides a high surface area and is beneficial for electrode performance. The SEM images of GO@SiO₂-NH₂-MIPs collected at different magnifications are given in Figures 5b and 5c. As shown in Figure 5b, a layer of MIP was covered on the GO@SiO₂-NH₂ sheets which indicated the successful MIP grafting on GO@SiO₂-NH₂ surface with high polymerization efficiency. It is obvious from these SEM images that NIPs have rough surface (Figure 5d), which is solely caused by the radical polymerization between the GO@SiO₂-NH₂ and cross-linker. However, due to the prearranged self-assembly of the template molecules and amino-functional GO in the presence of a porogenic solvent, the surface of GO@SiO₂-NH₂-MIPs exhibits more porosity and roughness in its structure than GO@SiO₂-NH₂-NIPs. This indicates

the presence of recognition sites in MIPs due to the removal of drug molecules, beneficial for higher adsorption rate and hence better performance of the electrode. The obtained EDX spectra of GO@SiO₂-NH₂-MIPs also confirm the FTIR and SEM results (Figure 6). The data obtained from energy dispersive spectroscopy (EDS) analysis of GO@SiO₂-NH₂ (figure not shown) and GO@SiO₂-NH₂-MIP/MWCNT/CPE showed the following atomic percentages, respectively: 52.14 wt.% (C), 15.07 wt.% (O), 13.70 wt.% (Si), 18.90 wt.% (N) and 62.53 wt.% (C), 19.02 wt.% (O), 6.13 wt.% (Si), 11.52 wt.% (N). These results clearly demonstrate the successful polymerization of GO@SiO₂-NH₂ and grafting of MIP on the surface of GO@SiO₂-NH₂.

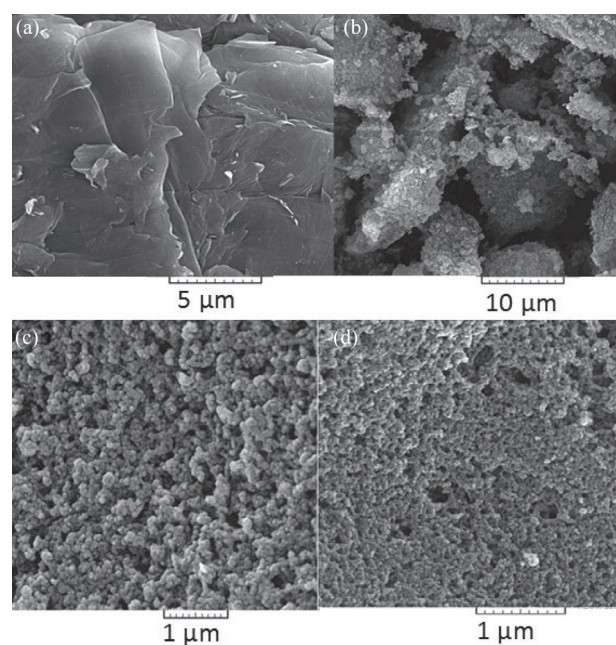


Figure 5. SEM images (a) of GO, and (b) and (c) of GO@SiO₂-NH₂-MIP at different magnification, and (d) of GO@SiO₂-NH₂-NIP.

Binding and recognizing properties of synthesized polymers

The recognition ability of the synthesized GO@SiO₂-NH₂-MIP and NIP was examined by batch rebinding experiments. In a typical binding assay, 0.01 g of MIP composite or its corresponding NIP was mixed with 10 mL of various concentrations of DIP in the range of 1–20 mg L⁻¹. After shaking for 30 min at 25 °C, the adsorption kinetics experiment done before showed that the adsorption could reach equilibrium in 30 min. The polymer composite particles were filtered off and the filtrate was analyzed for DIP by HPLC-UV detection. The quantity of the compound in solution was determined by reference to a standard calibration curve. By evaluation of these data, Q_c (amount of the DIP bound on the polymer composite

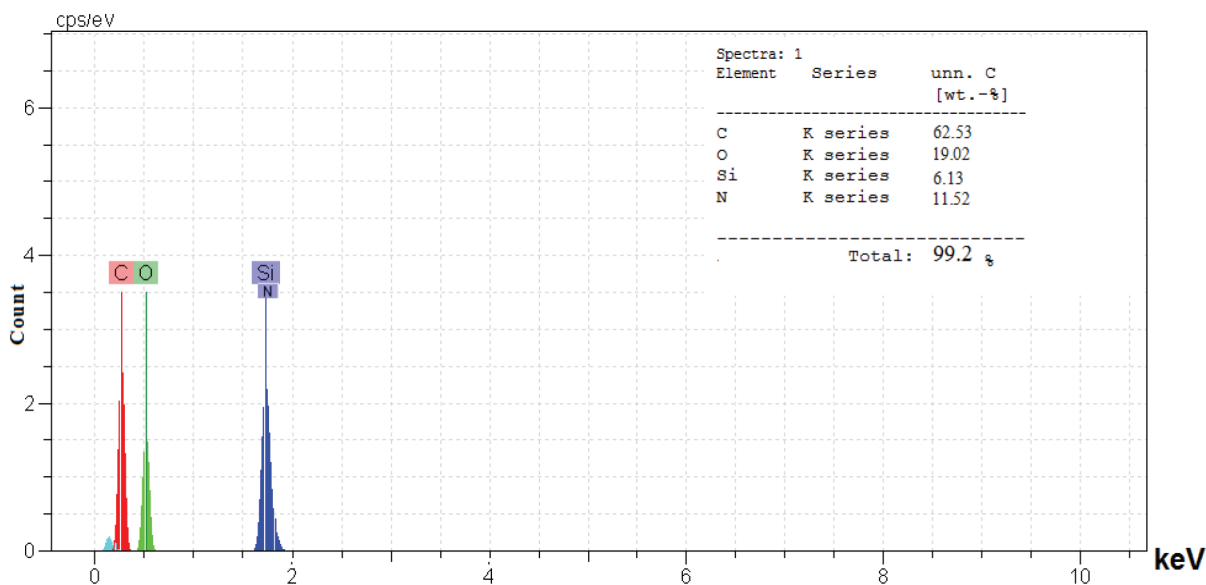


Figure 6. EDX analysis of GO@SiO₂-NH₂-MIP.

at equilibrium (60 min)) and K_d (distribution coefficient)³⁷ were calculated according to equations 1 and 2:

$$Q_e = (C_0 - C_e) V / w \quad (1)$$

$$K_d = Q_e / C_e \quad (2)$$

where Q_e (in mg g⁻¹), C_0 (in mg L⁻¹), and C_e (in mg L⁻¹) are the concentration of analyte initially and at equilibrium time, respectively, V (in mL) is the volume of the sample solution, and w (in g) is the mass of the polymer used.

The imprinting factors (I_F) of synthesized GO@SiO₂-NH₂-MIP was defined as the ratios of distribution coefficients³⁷ of analyte between the MIP and NIP composite and calculated according to equation 3:

$$I_F = K_{MIP} / K_{NIP} \quad (3)$$

The results demonstrated that the amount of Q_{MIP} toward DIP was much higher than Q_{NIP} . The I_F value was thus calculated as 10.1 for DIP on MIP. The large I_F indicates that the MIP sensor has great quantities of recognition sites for DIP. This confirms that in the binding process, DIP is strongly bound by imprinted polymers due to specific recognition sites which were formed on MIP.

Optimization of the carbon paste electrode composition and modification

The operating characteristics of ion selective electrodes can be significantly modified by changing the relative composition of the electrode components in which each component plays a special role in the electrode performance

and response. It has been well-known that characteristics of the potentiometric CPEs, such as the properties of the binder, the binder/graphite powder ratio and particularly the nature and the amount of the sensing materials used greatly influence the sensitivity, linear dynamic range and selectivity.³⁸ Thus, in order to obtain best performance, some GO@SiO₂-NH₂-MIP/MWCNT/CPE with different compositions, GO@SiO₂-NH₂-NIP/MWCNT/CPE and bare CPE were prepared and evaluated, and the results are summarized in Table 1.

As seen in Table 1, the sensor without GO@SiO₂-NH₂-MIPs modifier (No. 1) showed very low potentiometric response towards DIP. It can simply see that an increase at the GO@SiO₂-NH₂-MIPs composite in the paste composition caused a slope increase of the calibration curve (No. 2-4). This indicates that DIP-MIP is the most important component in the suggested electrode for sensing of DIP. In addition, a further increase in the MIP composite shows a decrease in the electrode performance, this may be due to the decreasing conductivity of electrode surface. For improving the potentiometric performance of GO@SiO₂-NH₂-MIPs/CPEs, MWCNTs can be as an excellent modifier for the modification of CPEs owing to their superior electrical conducting ability and high specific surface area. In this study, MWCNTs were used into the carbon paste that increased the available surface area and improved the conductivity properties of the electrode surface, and therefore, the conversion of the chemical signal to an electrical one. The obtained results indicated that the best potentiometric response was obtained for 10.0 wt.% of the MWCNTs in the presence of 12 wt.% of GO@SiO₂-NH₂-MIPs modifier. MWCNTs at 10 wt.% was

Table 1. Optimization of the carbon paste electrode composition and modification

No.	Composition / %				Slope / (mV dec ⁻¹)	Linear range / μM [DIP]
	Graphite	GO@SiO ₂ -NH ₂ -MIP	MWCNT	Binder		
1	75	0	0	25	10.3	–
2	70	10	0	20	51.2	2.0×10^{-6} - 2×10^{-5}
3	69	10	5	21	54.3	2.5×10^{-7} - 6.3×10^{-4}
4	50	15	10	25	57.4	5×10^{-8} - 1.0×10^{-3}
5	50	20	10	20	54.6	2.0×10^{-6} - 8.0×10^{-4}
6	55	12	10	23	59.41	2.5×10^{-8} - 1.1×10^{-2}
7	57	12	8	23	57.9	4.0×10^{-8} - 2.5×10^{-3}
8	50	13	12	25	61.1	6.3×10^{-8} - 6.4×10^{-4}
NIP ^a	50	12 ^a	12	23	9.664	–

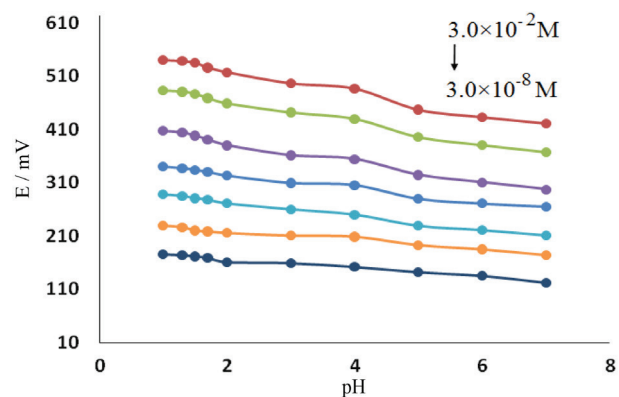
^aModifier is GO@SiO₂-NH₂-NIP/MWCNT/CPE; DIP: dipyrindamole; GO: graphene oxide; MIP: molecularly imprinted polymer; MWCNT: multi-walled carbon nanotube; NIP: non-imprinted polymer.

kept to avoid any mechanical problems within the electrode. Finally, as shown in Table 1, the electrode composed of 12.0% GO@SiO₂-NH₂-MIPs, 10.0% MWCNTs, 55.0% graphite powder and 23% silicon oil (electrode No. 6) was selected as the optimal ingredient composition for the analyte sensing.

Effect of pH on potentiometric response of DIP sensor

The potential of the sensing electrode is closely related to the charge and solubility of the analyte, it is highly dependent on the solution pH, and the testing medium pH is an important parameter to enhance the response of the electrode. The pH influence of the test solution on the potential response of the proposed sensor at different DIP concentrations (3.0×10^{-8} - 3.0×10^{-2} M) over the pH range of 1.0-7.0 was studied. The solution pH was gradually increased over the pH range from 1.0 to 7.0 using 2.0 mol L⁻¹ HCl and/or 0.1-1.0 mol L⁻¹ NaOH solution. The results were shown in Figure 7. The DIP maximum solubility is in acidic media, whereas increasing the pH of the medium solubility was decreased, and immediate lump formation of the drug was found in pH 6.8 indicating remarkable difference in drug solubility. Sink conditions occur when the amount of drug that can be dissolved in the dissolution medium is three times greater than the amount of drug to be dissolved.³⁹ In addition, as pH levels are beyond this range, the binding ability of the imprinted modifier for DIP molecule will become poor because of changes of molecule forms of host and guest. As it can be seen, the electrode potential was approximately pH independent in the range of 1.8-3.0. This can be taken as the working pH range of the electrode. Subsequently, in the DIP determination processes, the solution pH values were adjusted at 2 when required. On the other hand, decrease in potentials above pH 4.0 would be presumably due to the

formation of the deprotonated DIP species (pK_a 6.8) and to gradually increasing the free form of DIP base in the test solution which was not sensed by CPE. Weakly basic drugs are highly soluble in acidic, at pH 1-3. Therefore, it is expected that DIP is ionized at low pH. In this working pH range of electrode, DIP will exist as soluble ion and the response of the electrode is due to this form of DIP. All subsequent measurements were therefore made in 0.05 mol L⁻¹ HCl. The selected media for further studies was a 0.05 M HCl solution.

**Figure 7.** Effect of pH on the electrode response at different concentration.

Response time

It is well known that the dynamic response time of a sensor is one of the most important factors in its evaluation. This property was examined at required time to achieve equilibrium response over the different concentrations in the range 2.5×10^{-8} - 1.1×10^{-2} M. Sensor response time was determined by measuring the time to reach a stable potential (± 1 mV) after the immersion of the sensor in DIP solutions each having a 10-fold concentration. The cell potential was measured every 20 s after electrode immersion in each solution, and it was found to be steady (within ± 1 mV) at

all tested concentration levels (Figure 8a). Small potential drifts of -0.11 and -0.22 mV min $^{-1}$ were observed at this range. Moreover, taking into consideration the IUPAC definition for the response time,⁴⁰ the time which elapses between the instant when an ion-selective electrode and a reference electrode (ISE cell) are brought into contact with a sample solution (or at which the activity of the ion of interest in solution is changed) and the first instant at which the slope of the cell potential *vs.* time plot (emf/time slope, $\Delta E/\Delta t$) becomes equal to a limiting value selected on the basis of the experimental conditions and/or requirements concerning the accuracy (e.g., 0.6 mV min $^{-1}$), it was also found to be 20 s at all tested concentration levels. Figure 8b shows the reaching to equilibrium in response time of GO@SiO $_2$ -NH $_2$ -MIP/MWCNT/CPE and stability of the potential reading in few seconds for two concentrations. The short response time of electrode (20 s) may be due to using of GO as support in the synthesized surface MIP, and also incorporation of MWCNTs in the prepared carbon paste of the sensor leads to an exceptional improvement in mechanical properties and surface area in comparison with graphite, which may be the reason for the fast response time.⁴¹

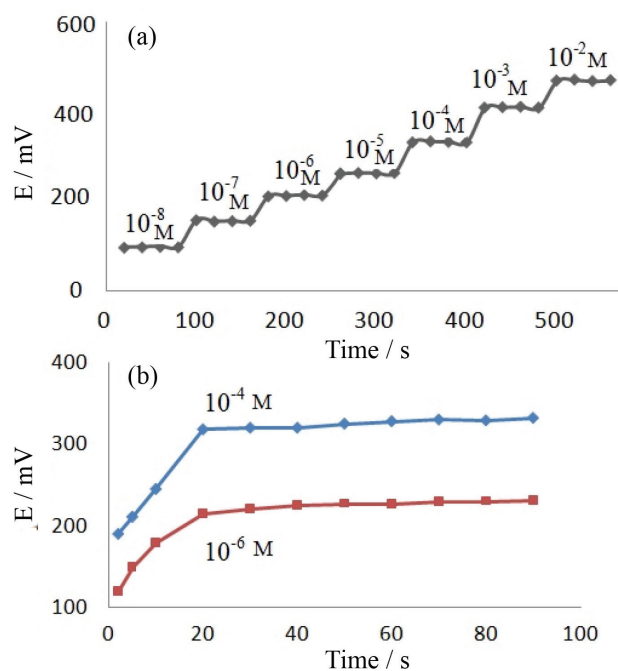


Figure 8. (a) Typical potential-time plot and (b) equilibrium time of the GO@SiO $_2$ -NH $_2$ -MIP/MWCNTs/CPE for response of sensor.

Potentiometric selectivity coefficients

The selectivity behavior is the most important characteristic of an ion selective electrode which determines the applicability of any sensor in the presence of foreign ions in the samples. Selectivity interprets relative electrode

response for the primary ion (A) over other species (B) that are present in the solution, being usually expressed in terms of potentiometric selectivity coefficient. The potentiometric selectivity coefficients were determined by the fixed interference method (FIM) (using 1.0×10^{-4} M concentration of both DIP and interfering species).^{42,43} The potential of a cell comprising an ion-selective electrode and a reference electrode is measured with solutions of constant level of interference ion, a_A , and varying activity of primary ion, a DIP. The potential values obtained are plotted *vs.* the concentration of the primary ion. The intersection of the extrapolation of the linear portions of this curve will indicate the value a_A which is to be used to calculate $K^{pot}_{A,B}$ from the following equation:

$$K_{A,B}^{Pot} = \frac{a_A}{(a_B)^{Z_A/Z_B}} \quad (4)$$

Z_A and Z_B are the charge numbers of the primary ion (A), and interfering ion (B), respectively; a_A and a_B are the activities of the primary and interfering ion. $K_{A,B}^{Pot}$ is the potentiometric selectivity coefficient for the primary ion against the interfering ion.

A selectivity factor below 1 indicates that the preference is for the primary ion, DIP. The resulting selectivity coefficients obtained for the proposed DIP-selective GO@SiO $_2$ -NH $_2$ -MIP/MWCNT/CPE were listed in Table 2. From the data given in Table 2, it is revealed that the proposed sensor has good selectivity toward DIP with respect to some ions, biological and tested drug. So, the disturbance produced by these species is negligible in the determination process of DIP in different samples. This is most probably due to the weak interaction between these interfering species and the GO@SiO $_2$ -NH $_2$ -MIP.

Table 2. Potentiometric selectivity coefficient values of GO@SiO $_2$ -NH $_2$ -MIP/MWCNT/CPE for dipyrindamole (DIP) detection

Interfering: X	$-\log K^{pot}_{DIP, X}$	Interfering: X	$-\log K^{pot}_{DIP, X}$
Aspirin	2.8	pyrrole	2.9
Glucose	4.5	urea	5.0
Caffeine	1.9	citrate	6.1
Ascorbic acid	3.8	K $^+$	2.1
Bipyridine	4.4	Fe $^{3+}$	3.4
Oxalic acid	3.6	Mg $^{2+}$	2.7
Atenolol	5.5	Ca $^{2+}$	4.6
Propranolol	4.3	NH $_4^+$	6.8
Salicylic acid	3.9	Cl $^-$	4.6

Response characteristics of the modified carbon paste sensor

Under optimal experimental conditions, the linearity of the proposed method was investigated by plotting the potential of the fabricated sensors (mV) as a function of logarithmic or responding concentration of the tested DIP. It has been shown that the fabricated sensors exhibit Nernstian response over the concentration range of 2.5×10^{-8} - 1.1×10^{-2} mol L⁻¹. Nernst factor is the slope of the DIP standard curve. In this research, the standard curve of DIP was obtained with the following linear regression equation: $y = -59.408 \text{ pDIP} + 587.7$ (Figure 9). Thus, in this study, the Nernst factor is $-59.408 \text{ mV dec}^{-1}$. The limit of detection of the DIP sensor was found to be approximately 1.1×10^{-8} M (signal/noise ratio of 3), which was based on IUPAC implication.⁴⁴ The calibration plots of GO@SiO₂-NH₂-MIP/MWCNTs/CPE and GO@SiO₂-NH₂-NIP/MWCNTs/CPE were compared. The obtained slope for non-imprinted composite modified carbon paste electrode was -9.664 . The result indicates that imprinting was successfully happened in the case of GO@SiO₂-NH₂-MIP/MWCNTs/CPEs. In contrast, for the non-imprinted electrode, as it is shown in Figure 9, the sensitivity of the NIP modified carbon paste electrode against DIP concentration variation is much lower than that of the MIP modified electrode.

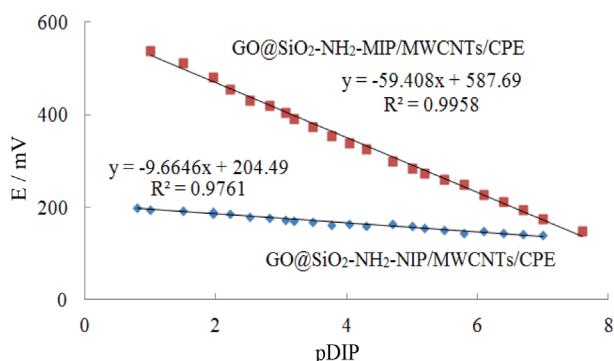


Figure 9. Calibration plots of GO@SiO₂-NH₂-MIP/MWCNTs/CPE and GO@SiO₂-NH₂-NIP/MWCNTs/CPE.

It is obvious that the use of GO@SiO₂-NH₂-MIP/MWCNTs/CPE improves the sensitivity for detection of very small DIP concentration. The better performance of the MIP-based potentiometric sensor is probably due to the specific interaction of DIP molecules with the recognition sites of MIP in the polymeric modifier. Evidently, it can be demonstrated that the MIP is effective for specific recognition of DIP. The average time required for the modified carbon paste electrode to reach a potential within ± 1 mV of the final equilibrium value after successive immersion of a series of DIP solutions, each having

10-fold difference in concentration, was less than 20 s over the entire concentration range and the potentials stayed constant after this time. However, the study presented here constitutes the first example of a potentiometric sensor for DIP which has surface MIPs as its recognition elements.

Reusability and life time of electrode

The reusability of the same MIP-based potentiometric sensor was evaluated by measuring the response potential of modified electrode 15 times in continuous experiments. The optimized electrode was used to measure DIP solution with concentration of 10^{-5} M; then, the Nernst factor and measurement range were determined. After each addition of DIP and the attainment of equilibrium, the electrode was regenerated by sequential washes with methanol/acetic acid (9:1, v/v) and deionized water until the initial potential obtained again. The results showed with usage up to 10 times, the obtained Nernst factor value is still quite good. In the usage of more than 11 times, the obtained Nernst factor is reduced. This decrease may be related to the memory effect due to the surface contamination. Hence, the electrode surface should be renewed to expose a fresh layer of modified paste ready for use after this phenomenon. In this electrode, a fresh surface was obtained by squeezing out a small amount of the paste, scrapping off the excess against a printing paper and polishing the electrode on a smooth paper to obtain a shiny appearance again. Therefore, a modified GO@SiO₂-NH₂-MIP/MWCNTs/CPE at optimum condition can be used for several months without any deterioration or change in the response of the electrode. The lifetime of the suggested selective sensor was evaluated for a period of 20 weeks by periodically recalibrating the potentiometric response to DIP in a series of DIP solutions. The obtained results showed that the proposed sensor can be used for at least 18 weeks (Figure 10a). After this time, a slight gradual decrease in the slope from -59.408 to $-58.230 \text{ mV dec}^{-1}$ is observed. The standard deviation of the potential responses every 5 min over a period of 2 h in a 1.0×10^{-3} M solution of DIP solutions was 0.7 mV ($n = 24$), revealing good stability of potential responses of the proposed electrode.

Electrode reversibility

The reversibility of the GO@SiO₂-NH₂-MIP/MWCNT/CPE was evaluated by alternated immersion of the electrodes into two stirred solutions of 10^{-3} and 10^{-5} M of DIP (Figure 10b). The proposed sensor represented a standard deviation of 0.9 mV for 4 replicate *per* each concentration level. This low standard deviation showed good reversibility and reproducibility of the fabricated DIP sensor exhibit. Therefore, electrode can be considered as a reusable electrode.

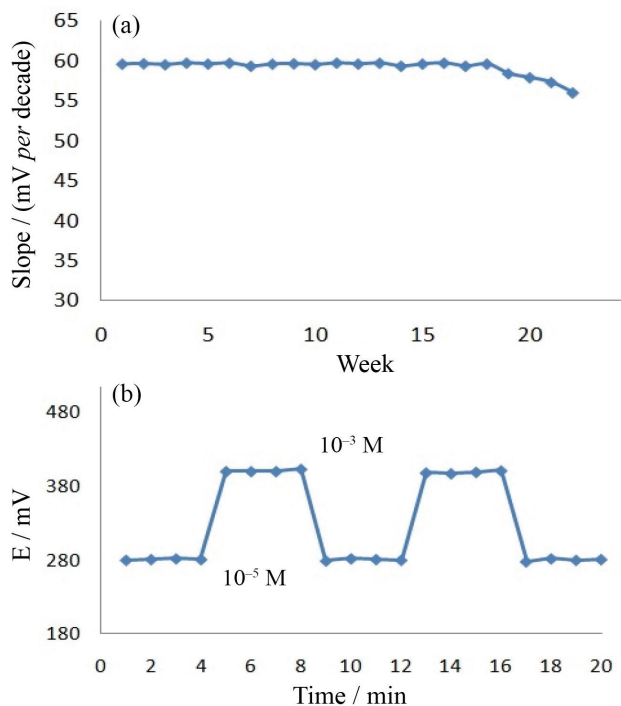


Figure 10. (a) Reusability and (b) reversibility of the GO@SiO₂-NH₂-MIP/MWCNTs/CPE for dipyrindamole (DIP) detection.

Sensor application to urine and pharmaceutical samples

In order to investigate the applicability of the constructed sensor to the determination of the drug in the real samples, DIP was determined in human urine samples and pharmaceutical tablets by the potentiometric method. The GO@SiO₂-NH₂-MIP/MWCNT/CPE was used for potentiometric determination of DIP in human urine of healthy individuals and that of samples from volunteers after injection of DIP tablet (each tablet contains 25 mg of DIP). Spiked and un-spiked urine samples were analyzed using GO@SiO₂-NH₂-MIP/MWCNT/CPE and potentiometric method. The samples were spiked with DIP at different concentration levels in the range of calibration curve, and DIP content of the solution was then determined by the proposed GO@SiO₂-NH₂-MIP/MWCNT/CPE, using the calibration method. Additionally, the electrode has been used for the DIP determination in solution of DIP tablets with satisfactory recoveries without any previous pretreatment or extraction. Stock solutions of the pharmaceutical compounds were obtained as mentioned in the experimental section, and these were subsequently diluted so that DIP concentration falls in the range of the calibration plot. The results are given in Table 3. The results reveal that the potentiometric method can be used for the DIP determination in pharmaceutical formulations and urine without interference by the excipients expected to be present in tablets or the constituents of urine. As demonstrated, the obtained recoveries are between 96.0 and

103.1% with RSD (relative standard deviation) less than 3.2%, indicating the acceptable accuracy and precision of the potentiometric determination of DIP using the proposed sensor. The DIP determination results for urine and pharmaceutical formulation using the proposed sensor were compared with those measured by HPLC-UV detection. The obtained results from pharmaceutical formulation were statistically evaluated by performing Student's *t*-test and *F*-test.⁴⁵ As can be seen in Table 4, the values calculated were found to be less than tabulated values at 95% confidence level indicating no significant differences in the accuracy and precision of the recommended method and the HPLC-UV.

Table 3. Application of the potentiometric procedure using GO@SiO₂-NH₂-MIP/MWCNT/CPE to the dipyrindamole (DIP) concentration measurements in urine samples and its comparison with the HPLC-UV analysis

Sample	Added / μM	Found ^a / μM (RSD / %), potentiometric	Recovery / %	Found ^a / μM (RSD / %), HPLC analysis
Urine 1				
	0	not detected	not detected	not detected
	10	9.6 (1.3)	96	9.4 (2.7)
	100	103.1 (1.6)	103.1	102.9 (2.5)
	1000	987 (2.6)	98.7	993 (3.1)
Urine 2				
	0	not detected	not detected	not detected
6 h	10	10.1 (3.1)	101.1	10.3 (2.5)
	100	98.0 (1.9)	98.0	97.8 (2.8)
12 h	0	4.6 (3.3)	–	4.7 (3.2)
	10	14.8 (1.6)	102.0	15.1 (3.0)
18 h	100	101.7 (2.6)	97.1	102.2 (2.8)
	0	2.29 (1.3)	–	2.43 (3.1)
18 h	10	12.1 (1.6)	99.0	12.9 (2.8)
	100	99.6 (2.6)	97.4	10.6 (2.4)

^aAverage of three determinations; RSD: relative standard deviation; HPLC-UV: high performance liquid chromatography-ultraviolet; urine 1: healthy urine samples without taking medication; urine 2: urine samples of a 60 years old male, collected after taking a 25 mg dipyrindamole tablet and collected at different intervals (6, 12 and 18 h).

Comparison of potentiometric methods using GO@SiO₂-NH₂-MIP/MWCNTs/CPE with previous method for analysis of DIP

A comparison between the analytical parameters of the suggested sensor and a few electrochemical electrodes reported in the literature for the DIP determination are given in Table 5.^{1,3,16,17} In this study, we conducted a comparison analysis of DIP using the potentiometric method with previous methods, such as differential pulse voltammetry and stripping voltammetry. The comparison results of these

Table 4. Comparison of dipyrindamole (DIP) assay in tablet formulations by means of the described potentiometric procedure using GO@SiO₂-NH₂-MIP/MWCNTs/CPE and the HPLC-UV method

Claimed value / mg per tablet	Added / mg	Found ^a / mg		<i>t</i> -test ^b	<i>F</i> -test ^c
		Potentiometric	HPLC		
25	–	24.6 ± 1.6 ^d	25.5 ± 1 ^d	2.2	2.56
25	10.0	36.1 ± 1.1 ^d	35.7 ± 1.2 ^d	0.42	0.84

^aAverage of 6 determinations; ^btabulated *t*-value for 5 degrees of freedom at 95% confidence level is 2.57; ^ctabulated *F*-value for (5, 5) degrees of freedom at 95% confidence level is 5.05; ^dmean ± standard deviation (n = 6); HPLC: high performance liquid chromatography.

Table 5. Comparison of potentiometric methods using GO@SiO₂-NH₂-MIP/MWCNTs/CPE with previous sensors for analysis of dipyrindamole (DIP)

Method / electrode	Modifier	LOD	Linear range	RSD / %	Reference
SWV / HMDE ¹	–	0.018 μM	1.28-7.02 μM	0.97	1
DPV / GCE ²	MIP/Fe ₃ O ₄ @Au-MWCNT	0.03 ng mL ^{-1a}	0.5-1900 ng mL ⁻¹	4.6	3
DPASV / CPE ³	MIP	0.05 ng mL ^{-1b}	1.0-110 ng mL ⁻¹	4.7	16
DPV / CPE ⁴	CTAB	0.01 μg mL ^{-1c}	0.03-12 μg mL ⁻¹	1.37	17
Potentiometric / CPE	GO@SiO ₂ -NH ₂ -MIP/MWCNT	0.011 μM	0.025-11000 μM	< 3.2	this work

^a0.00005 μM; ^b0.0001 μM; ^c0.02 μM; LOD: limit of detection; RSD: relative standard deviation; SWV / HMDE: square wave voltammetry at a hanging mercury drop electrode; DPV / GCE: differential pulse voltammetry at a glassy carbon electrode; DPASV / CPE: differential pulse adsorptive stripping voltammetry at a carbon paste electrode; DPV / CPE: differential pulse voltammetry at a carbon paste electrode.

methods showed that each method has advantages and disadvantages. The potentiometric method has wider linear range and good precision, but some of the voltammetric methods have lower LOD values than the potentiometric method.

However, the most important advantage of this innovative sensing platform is its highest resistance against the interference effect of the most serious interfering targets, such as ascorbic acid and aspirin, among the represented determination methods. Potentiometric detection of DIP with constructed ion selective electrode can be a fast, cheap and easy technique compared with some of the reported voltammetric methods, besides it is characterized by high precision and accuracy than methods mentioned above. The sensor is characterized by a high selectivity with respect to some ions as indicated by the selectivity coefficient values given in Table 3.

Conclusions

This is the first report in which graphene oxide based dipyrindamole surface molecularly imprinted polymers with high affinity and selectivity for dipyrindamole were prepared and used as synthetic recognition elements of a potentiometric sensor. In this work, we have constructed a highly selective DIP electrode based on amino silica graphene oxide DIP imprinted polymer as the molecule recognition material in MWCNT/CPE matrix. Owing to utilizing the GO@SiO₂-NH₂-MIP besides MWCNTs in the

carbon paste composition, the propounded sensor compared with previously reported DIP sensors offers preponderantly attractive advantageous, especially, in terms of the selectivity over some foreign compounds. A comparison of the proposed electrode with reported electrodes shows that the proposed electrode is better than most reported sensors in terms of working concentration range, LOD and response time. High sensitivity, stability, selectivity and low LOD (1.1×10^{-8} M) make this electrode suitable for measuring the DIP concentration in a variety of samples without the need for pre-treatment steps and without significant interactions from other species present in the samples. In fact, the sensor configuration and the analytical technique described here allow a simple and low cost method for DIP determination in pharmaceuticals and biological fluids. Furthermore, synthetic recognition elements such as MIPs can be prepared when there are no corresponding biological alternatives such as antibodies.

Acknowledgments

The authors greatly appreciate the financial support of this work by Shahid Chamran University of Ahvaz Research Council.

References

- de Toledo, R. A.; Castilho, M.; Mazo, L. H.; *J. Pharm. Biomed. Anal.* **2005**, *36*, 1113.

2. Balakumar, P.; WitnessKoe, W. E.; Gan, Y. S.; JemayPuah, S. M.; Kuganesswari, S.; Prajapati, S. K.; Varatharajan, R.; Jayachristy, S. A.; Sundram, K.; Bahari, M. B.; *Regul. Toxicol. Pharmacol.* **2017**, *84*, 35.
3. Liu, X.; Zhong, J.; Rao, H.; Lu, Z.; Ge, H.; Chen, B.; Zou, P.; Wang, X.; He, H.; Zeng, X.; Wang, Y.; *J. Solid State Electrochem.* **2017**, *21*, 3071.
4. Humphreys, D. M.; Street, J.; Schumacher, H.; Bertrand-Hardy, J. M.; Palluk, R.; *Int. J. Clin. Pract.* **2002**, *56*, 121.
5. Pulgarin, J. A. M.; Molina, A. A.; Lopez, P. F.; *Anal. Biochem.* **1997**, *245*, 8.
6. Salinas-Castillo, A.; Carretero, A. S.; Fernández-Gutiérrez, A.; *Anal. Bioanal. Chem.* **2003**, *376*, 1111.
7. Shoukry, A. F.; Ghani, A. N. T.; Issa, Y. M.; Wahdan, O. A.; *Anal. Lett.* **2001**, *34*, 1689.
8. Zhu, G.; Ju, H.; Zheng, H.; *Clin. Chim. Acta* **2004**, *348*, 101.
9. Rouhi, M.; Pourbasheer, E.; Ganjali, M. R.; *Monatsh. Chem.* **2015**, *146*, 1593.
10. Chena, M.; Granvil, C.; Ji, Q. C.; Zhang, Z. Y.; Padval, M. V.; Kansra, V. V.; *J. Pharm. Biomed. Anal.* **2009**, *49*, 1241.
11. Liu, D.; Wang, R. H.; Nie, L. H.; Yao, S. Z.; *J. Pharm. Biomed. Anal.* **1996**, *14*, 1471.
12. Wang, Z.; Zhang, H.; Zhou, S.; *Talanta* **1997**, *44*, 621.
13. Rao, Z. M.; Zhang, W. H.; Li, Q. Z.; Xie, G. P.; Yang, H. Q.; *Spectrosc. Spectral Anal.* **2004**, *24*, 278.
14. Wang, L.; Zhang, Z.; *Sens. Actuators, B* **2008**, *133*, 40.
15. Nishitani, A.; Tsukamoto, Y.; Kanda, S.; Imai, K.; *Anal. Chim. Acta* **1991**, *251*, 241.
16. Javanbakht, M.; Fathollahi, F.; Divsar, F.; Ganjali, M. R.; Norouzi, P.; *Sens. Actuators, B* **2013**, *182*, 362.
17. Li, C.; *Colloids Surf., B* **2007**, *55*, 77.
18. Wang, N.; Xu, F.; Zhang, Z.; Yang, C.; Sun, X.; Li, J.; *Biomed. Chromatogr.* **2008**, *22*, 149.
19. Qin, T.; Qin, F.; Li, N.; Lu, S.; Liu, W.; Li, F.; *Biomed. Chromatogr.* **2010**, *24*, 268.
20. Parsaei, M.; Asadi, Z.; Khodadoust, S.; *Sens. Actuators, B* **2015**, *220*, 1131.
21. Sun, L.; Sun, C.; Sun, X.; *Electrochim. Acta* **2016**, *220*, 690.
22. Gandía-Romero, J. M.; Campos, I.; Valcuende, M.; García-Brejijo, E.; Marcos, M. D.; Pay, J.; Soto, J.; *Cem. Concr. Compos.* **2016**, *68*, 66.
23. Yin, T.; Qin, W.; *TrAC, Trends Anal. Chem.* **2013**, *51*, 79.
24. Abdel-Ghany, M. F.; Hussein, L. A.; El Azab, N. F.; *Talanta* **2017**, *164*, 518.
25. Huang, X.; Wei, S.; Yao, S.; Zhang, H.; He, C.; Cao, J.; *J. Pharm. Biomed. Anal.* **2019**, *164*, 607.
26. Gao, B.; Liu, H.; Cui, K.; *Sens. Actuators, B* **2018**, *254*, 1048.
27. Darmokoesoemo, H.; Kustyarini, L.; Kadmi, Y.; Khasanah, M.; Kusuma, H. S.; Elmsellem, H.; *Results Phys.* **2017**, *7*, 1781.
28. Bompert, M.; Haupt, K.; Ayela, C.; *Top. Curr. Chem.* **2012**, *325*, 83.
29. Huang, J.; Wu, Y.; Cong, J.; Luo, J.; Liu, X.; *Sens. Actuators, B* **2018**, *259*, 1.
30. Liu, S.; Pan, J.; Zhu, H.; Pan, G.; Qiu, F.; Meng, M.; Yao, J.; Yuan, D.; *Chem. Eng. J.* **2016**, *290*, 220.
31. Li, D.; Müller, M. B.; Gilje, S.; Kaner, R. B.; Wallace, G. G.; *Nat. Nanotechnol.* **2008**, *3*, 101.
32. O'Neil, G. D.; Fouskaki, M.; Kounaves, S. P.; Chaniotakis, N. A.; *Electrochem. Commun.* **2015**, *55*, 51.
33. Saadati, F.; Ghahramani, F.; Shayani-jam, H.; Piri, F.; Yaftian, M. R.; *J. Taiwan Inst. Chem. Eng.* **2018**, *86*, 213.
34. Mirzajani, R.; Karimi, S.; *Ultrason. Sonochem.* **2019**, *50*, 239.
35. Alvarez-Lorenzo, C.; Concheiro, A.; *Handbook of Molecularly Imprinted Polymers*; Smithers Rapra: London, UK, 2013.
36. Dadkhah, S.; Ziaei, E.; Mehdinia, A.; Kayyal, T. B.; Jabbari, A.; *Microchim. Acta* **2016**, *183*, 1933.
37. Gao, B.; Liu, H.; Cui, K.; *Sens. Actuators, B* **2018**, *254*, 1048.
38. Bagheri, H.; Shirzadmehr, A.; Rezaei, M.; *J. Mol. Liq.* **2015**, *212*, 96.
39. Anilkumar, A.; Murthy, T. E. G. K.; Rani, A. P.; *Indian J. Pharm. Educ. Res.* **2018**, *52*, 374.
40. Zhang, W.; Xu, Y.; Zou, X.; *Food Chem.* **2018**, *261*, 1.
41. Borini, S.; White, R.; Wei, D.; Astley, M.; Haque, S.; Spigone, E.; Harris, N.; Kivioja, J.; Ryhänen, T.; *ACS Nano* **2013**, *7*, 11166.
42. Mazloum Ardakani, M.; Pourhakkak, P.; Salavati-Niasari, M.; *J. Braz. Chem. Soc.* **2007**, *18*, 782.
43. Bakker, E.; Pretsch, E.; Bühlmann, P.; *Anal. Chem.* **2000**, *72*, 1127.
44. Abdel-Ghany, M. F.; Hussein, L. A.; El Azab, N. F.; *Talanta* **2017**, *164*, 518.
45. Mirzajani, R.; Ramezani, Z.; Kardani, F.; *Microchem. J.* **2017**, *130*, 93.

Submitted: December 31, 2018

Published online: May 16, 2019

